Ann. Geophys., 29, 1939–1954, 2011
www.ann-geophys.net/29/1939/2011/
doi:10.5194/angeo-29-1939-2011

Annales Geophysicae

Characteristics of Arctic tides at CANDAC-PEARL (80° N, 86° W) and Svalbard (78° N, 16° E) for 2006–2009: radar observations and comparisons with the model CMAM-DAS

A. H. Manson[1], **C. E. Meek**[1], **X. Xu**[1], **T. Aso**[2], **J. R. Drummond**[3], **C. M. Hall**[4], **W. K. Hocking**[5], **M. Tsutsumi**[2], **and W. E. Ward**[6]

[1]Institute of Space and Atmospheric Studies, University of Saskatchewan, Saskatoon, Canada
[2]National Institute for Polar Research, Tokyo, Japan
[3]Physics and Atmospheric Science Department, Dalhousie University, Halifax, Canada
[4]Tromsø Geophysical Observatory, University of Tromsø, Tromsø, Norway
[5]Physics and Astronomy Department, University of Western Ontario, London, Canada
[6]Physics and Astronomy Department, University of New Brunswick, Fredericton, Canada

Received: 17 June 2010 – Revised: 14 September 2011 – Accepted: 25 September 2011 – Published: 31 October 2011

Abstract. Operation of a Meteor Radar (MWR) at Eureka, Ellesmere Island (80° N, 86° W) began in February 2006: this is the location of the Polar Environmental and Atmospheric Research Laboratory (PEARL), operated by the "Canadian Network for the Detection of Atmospheric Change" (CANDAC). The first 36 months of tidal wind data (82–97 km) are here combined with contemporaneous tides from the Meteor Radar (MWR) at Adventdalen, Svalbard (78° N, 16° E), to provide the first significant evidence for interannual variability (IAV) of the High Arctic's diurnal and semidiurnal migrating (MT) and non-migrating tides (NMT).

The three-year monthly means for both diurnal (DT) and semi-diurnal (SDT) winds demonstrate significantly different amplitudes and phases at Eureka and Svalbard. Typically the summer-maximizing DT is much larger ($\sim$24 m s^{-1} at 97 km) at Eureka, while the Svalbard tide (5–24 m s^{-1} at 97 km)) is almost linear (north-south) rather than circular. Interannual variations are smallest in the summer and autumn months. The High Arctic SDT has maxima centred on August/September, followed in size by the winter features; and is much larger at Svalbard (24 m s^{-1} at 97 km, versus 14–18 m s^{-1} in central Canada). Depending on the location, the IAV are largest in spring/winter (Eureka) and summer/autumn (Svalbard).

Fitting of wave-numbers for the migrating and non-migrating tides (MT, NMT) determines dominant tides for each month and height. Existence of NMT is consistent with nonlinear interactions between migrating tides and (quasi) stationary planetary wave (SPW) $S = 1$ (SPW1). For the diurnal oscillation, NMT $s = 0$ for the east-west (EW) wind component dominates (largest tide) in the late autumn and winter (November–February); and $s = +2$ is frequently seen in the north-south (NS) wind component for the same months. The semi-diurnal oscillation's NMT $s = +1$ dominates from March to June/July. There are patches of $s = +3$ and $+1$, in the late fall-winter. These wave numbers are also consistent with SPW1-MT interactions.

Comparisons for 2007 of the observed DT and SDT at 78–80° N, with those within the Canadian Middle Atmosphere Model Data Assimilation System CMAM-DAS, are a major feature of this paper. The diurnal tides for the two locations have important similarities as observed and modeled, with seasonal maxima in the mesosphere from April to October, and similar phases with long/evanescent wavelengths. However, differences are also significant: observed Eureka amplitudes are generally larger than the model; and at Svalbard the modeled tide is classically circular, rather than anomalous. For the semi-diurnal tide, the amplitudes and phases differ markedly between Eureka and Svalbard for both MWR-radar data and CMAM-DAS data. The seasonal variations from observed and modeled archives also differ at each location. Tidal NMT-amplitudes and wave-numbers for the model differ substantially from observations.

Keywords. Meteorology and atmospheric dynamics (Middle atmosphere dynamics; Polar meteorology; Waves and tides)

Correspondence to: A. H. Manson
(alan.manson@usask.ca)

Published by Copernicus Publications on behalf of the European Geosciences Union.

1 Introduction

The first comprehensive paper on tidal characterizations in the northern High Arctic (Manson et al., 2009, Paper 1), provided analyzed data (12 months of 2006/2007) from the Meteor Wind Radars (MWR) at Adventdalen, Svalbard (78° N, 16° E) and Eureka, Ellesmere Island (80° N, 86° W). There had been modest optical observations from Eureka, and radar observations (65–70° N) from Europe, Scandinavia and Alaska (Portnyagin et al., 2004; Manson et al., 2004c; and Wu et al., 2003); and a substantial data-archive and papers from Continental Antarctica exists (e.g. Hernandez et al., 1993; Forbes et al., 1995; Portnyagin et al., 1998). No additional "80° N" radars have been installed in the interim e.g. in the desirable Russian Arctic Islands. However satellite Arctic tidal data from the TIDI system (TIMED Doppler Interferometer) were published while this paper was in review (Iimura et al., 2010), and brief remarks of a comparative nature are included in our "Summary and Discussion". For this paper, we had already chosen to compare tides from the first three years of data (2006–2009) resulting from operation of the Eureka and Svalbard MWR radars, with a general circulation model (GCM) with a data assimilation system: Canadian Middle Atmosphere Model, CMAM-DAS (Ren et al., 2008).

The presence of NMT in the High Arctic of 2006/2007, as indicated in the studies summarized within Manson et al. (2009), were shown by us to be consistent with the paper by Forbes and Wu (2006). It is important to realize that there are limitations to the value of such comparisons due to some differences in the latitudinal structures of the temperature and wind tides (Manson et al., 2010). E.g. Features in wind-spectra typically extend to higher latitudes. However inspection of the 70° N temperature-tides from UARS-MLS (Forbes and Wu, 2006), and wave-number plots from CMAM-DAS (Xu et al., 2011a, b; Manson et al., 2010), show generally similar characteristics, with typically weak amplitudes at the high Arctic latitudes for the MT and their relatively even weaker NMT. Comparisons of the tidal winds (2006–2009) from the two High Arctic radars and CMAM-DAS at ∼80° N are thus an important feature of this present paper.

It has been our intention, as a goal of CANDAC-PEARL's IPY program, to also investigate the inter-annual variations (IAV) of the MT and NMT at Svalbard and Eureka. . . hence this is also a major focus of the present paper. There are certainly physical expectations for IAV based upon variable forcing mechanisms e.g. the SPW, and already good evidence that interannual variations may be significant (Hagan and Forbes, 2003; Baumgaertner et al., 2005, 2006; Wu et al., 2008).

Possible relationships between the occurrences and variabilities of SPW and the global morphology of the NMT of the diurnal and semidiurnal tides were subjected to preliminary study in Paper 1. There was little to no indication of significant diurnal NMT forcing (in the Arctic) from the Southern Hemisphere's winter SPW. Regarding the semidiurnal tide, it was considered probable, and since then demonstrated clearly by Xu et al. (2009a, c), that the large SPW of the NH winter and their associated NMT are linked through trans-equatorial propagation to the observed summer SDT at Rothera in Antarctica. It was proposed to use a GCM model with data assimilation for comparisons with the observed and calculated NMT in future studies: this is also a major feature of the present paper.

We recognize the complementary Southern Hemisphere (SH) studies, which use the geographically attractive Antarctic continent for observational sites along the coast from 68–78° S and also centered at the pole ("South Pole" station). Portnyagin et al. (1998), Murphy et al. (2006, 2009) and Baumgaertner et al. (2005, 2006) used a variety of radar-combinations to illustrate the presence and at times dominance of the semidiurnal tide's NMT $s = +1$ during their summer-equinox months). In causal relation to this they variously suggested or demonstrated that the amplitudes of the Arctic's NMT and SPW $S = +1$ were positively correlated during the NH-winter months, when the $S = +1$ SPW is also dominant in Antarctica (see also Paper 1).

The radars and model are briefly described in Sect. 2. The focus of Sect. 3 is the unique formation of the first height (82–97 km) versus time (12 months using means from 2006–2009) contour plots of the radar-derived diurnal (DT) and semidiurnal (SDT) tidal amplitudes and phases at the two High Arctic (effectively equal) latitudes and differing longitudes (16° E and 86° W). Variations in the mesospheric Arctic tides (circa 80–100 km) over three years, or inter-annual variations (IAV), which were heretofore not available, are also provided and discussed. The topic of IAV in the occurrence or importance of Arctic NMT, another unknown, is addressed with figures (height versus month plots for each of 3 years) that provide the relative magnitudes of the migrating and non-migrating tides (MT, NMT). The purpose of Sect. 4 is to effectively compare and contrast, for the first time, the observed tides from Eureka and Svalbard for a year (2007), with the modeled products from the "state of the art" spectral CMAM-DAS. Contour plots (height versus month) of tidal amplitudes and phases, as well as plots of relative magnitudes of NMT and MT for each of the three years, are provided. In Sect. 5, the focus is upon spatial wave-numbers for the NMT of CMAM-DAS and their IAV. The Summary and Discussions, which address the progress achieved in addressing the above goals, are in Sect. 6.

2 Meteor radar winds and the atmospheric model CMAM-DAS

We use two MWR (Meteor Wind) radars of similar design (Hall et al., 2003; Hocking and Hocking, 2002). Commercially the radar at Eureka (80° N, 86° W) is known as a

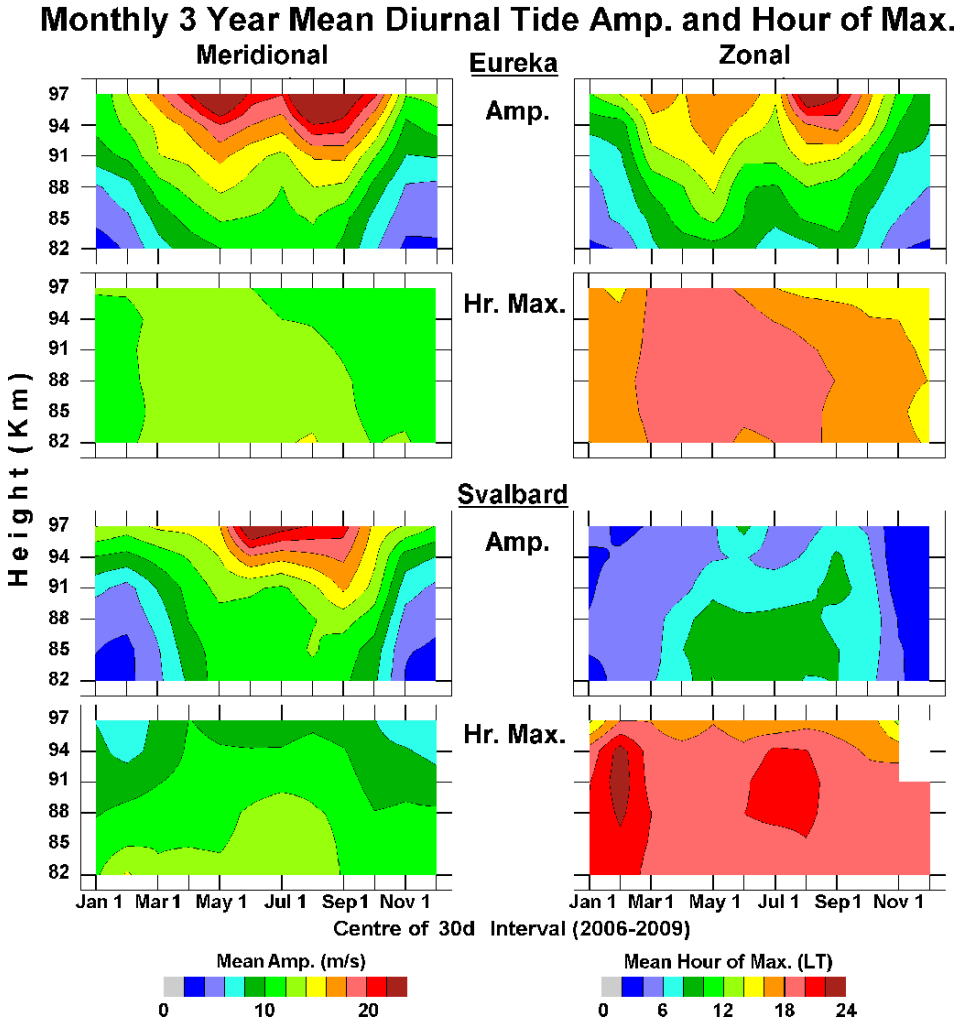

Fig. 1. Zonal (U, EW) and meridional (V, NS) winds for the diurnal (24-h) tides above Eureka and Svalbard for days February 2006–February 2009; the phases are the local solar times of maximum northward and eastward winds. Separate averaging for amplitudes and phases was done for the tides, and if the phase-spread between the values from three years exceeds 180° for an interval, a phase-gap is shown. 30-day fits are used, with the first day of the calendar month as the middle of the 30-day data sets.

SKiYMET system, which was developed and deployed by MARDOC-Incorporated (Modular Antenna Radar Designs of Canada). The Svalbard (78° N, 16° E) radar was built by Atmospheric Radar [ATRAD] Systems Pty Ltd of Adelaide. More details have been included in Manson et al. (2009, 2011).

The unique spectral Canadian Middle Atmosphere Model (CMAM, e.g. Manson et al., 2006) has been a valuable research system for us, allowing collaborative and comparative studies of mutual benefit for the professors involved. At this time the Data Assimilation System (DAS) has been developed as an option (Ren et al., 2008) and data from the IPY years are used here as specified in the last paragraph of the Introduction.

3 Diurnal tides (2006–2009): migrating (MT) and non-migrating (NMT); comparisons with CMAM-DAS for 2007

3.1 Introduction

The "monthly 3 year" amplitudes and phases of the diurnal (24-h) tides (DT) at both locations are provided in Fig. 1, with their "monthly 3 year variations" in Fig. 2. Northward and eastward tidal winds are taken as positive; and the phases (local solar times) provided are those of maximum northward and eastward winds. The corresponding information for the semidiurnal (12-h) tides will be treated later. The "variation of amplitudes" and "variation of phase-hours" which are our measures of IAV are provided in Fig. 2, with their definition being in the caption. Separate averaging for amplitudes and

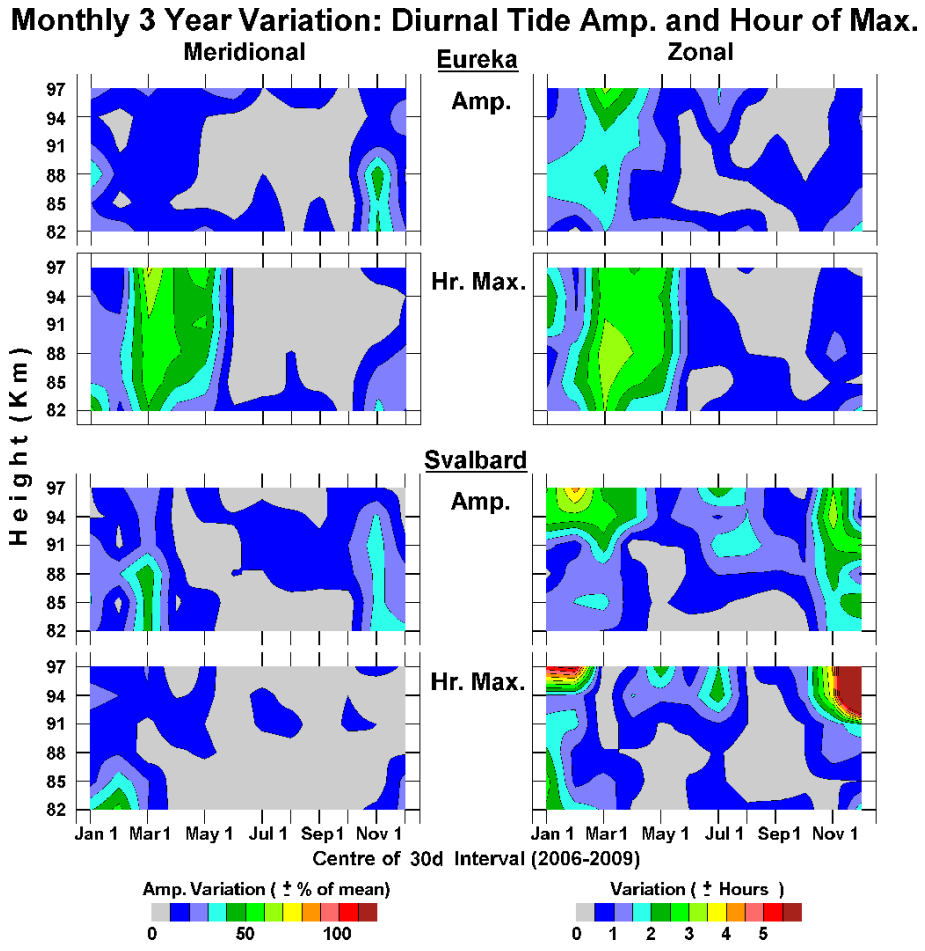

Fig. 2. The "variation" of 24-h tidal amplitudes and phases (local times of maximum), over three years (February 2006 to February 2009), are provided. The "variation" of amplitude is: [100(maximum − minimum)/(maximum + minimum)] %, and of phase in hours is: [(maximum − minimum)/2]. Separate calculations for amplitudes and phases were done for the tides.

phases was done for the tides, and if the phase-spread between the values from three years exceeds 180°, for a month, a phase-gap is shown. This latter rarely occurred.

3.2 Diurnal tides: means, variations and NMT features

For the 2006–2009 interval at Eureka (Fig. 1) the DT amplitude minima are in winter-centered months (October–November to February–March), with broad maxima (increasing with height) between, which includes sub-maxima centered on April–May and August. The Eureka phases (Fig. 1) are consistently orthogonal (6 h differences between meridional and zonal components), and wind-maxima occur at later hours during the summer. Minima in amplitude and phase variations (Fig. 2) occur in months of these amplitude maxima: minimal IAV from June to the end of autumn, small in winter and notably largest in the spring (late-February to May). For example these latter months of 2006 (Paper 1, Fig. 4) had significant differences in phase (4–6 h later in LT) and amplitude (4–6 m s^{-1} larger) from the 3 year means.

Turning to the Svalbard DT in Fig. 1, seasonal patterns of amplitude and phase are significantly different from those at Eureka and actually rather similar to that in 2006/2007 (Paper 1). The tide is not circularly polarized, as the amplitudes of the EW component are relatively small in summer-centred months. Generally, the lower thermospheric Svalbard DT is much weaker than that at Eureka. Phases for EW and NS components (Fig. 1) demonstrate modest temporal differences compared with Eureka, while changes with height are more apparent over the year, and consistent with descending tidal phase propagation. "Variations" of both types (Fig. 2), as our indicators of IAV, are again smallest in summer-centred months, but the spring months show almost none of the activity visible at Eureka.

The mean DT amplitudes and phases for 2006–2009 are consistent with significant non-migrating tide (NMT) effects. The amplitudes at very similar latitudes (78, 80° N) are frequently different, and the phases (local times) are close to identical for only limited months and heights. A "two-tide

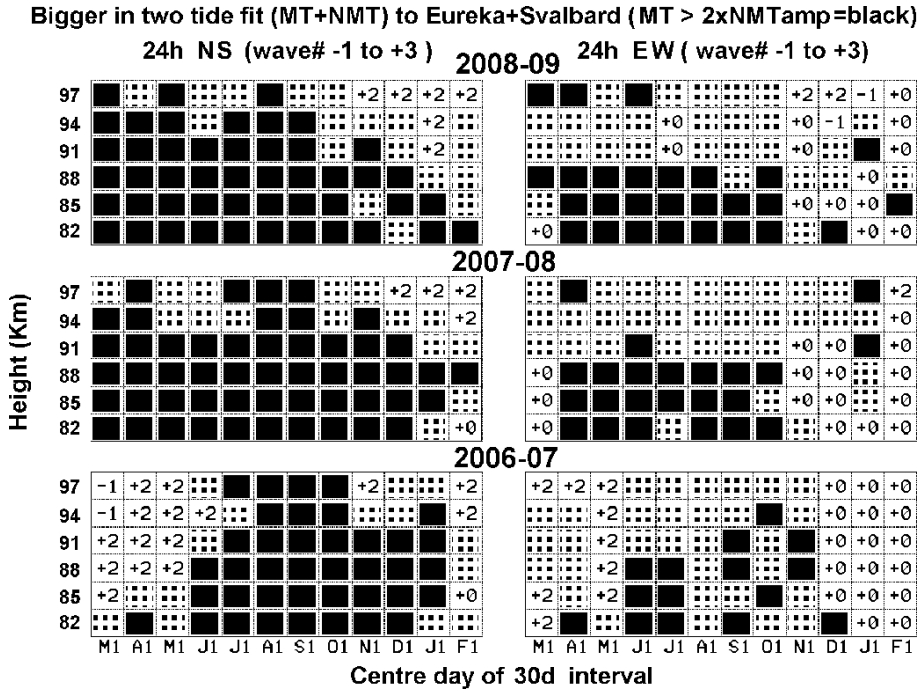

Fig. 3. Two-tide fits, using the wave number of the diurnal MT ($s = 1$) plus one of a range of NMT, were used to find the relative sizes: a black square is chosen if MT is greater than twice any NMT value; a grey square is chosen when one or more NMT values are smaller then MT, but greater than 0.5 of MT; the wave-number "*s*" is chosen that has the largest NMT [relative to the corresponding MT amplitude] of all of the fits. Wave-numbers ($s = -1$ to $+3$) are appropriate to non-linear interaction of the diurnal MT with the SPW $S = 1$ or 2.

fit" was used in Paper 1, and is used here with minor change, in which the migrating 24-h tide and one of a selection of non-migrating tides are fitted to the monthly data from the two radar sites. The justification for its use is simply because of the previous good results, with no indication of noise or inconsistencies. We provide here a brief summary of the methodology and any assumptions that are inherent. As described in detail in Manson et al. (2009), the method for determining whether the migrating tide dominates, and if not, which NMT is largest, is to solve for the MT and an NMT simultaneously. There are no degrees of freedom remaining (two known for each of the observed tides at the radars; two solutions for each of the MT and chosen NMT) to identify the best fit by minimum squared error, but it is expected that if one tide dominates significantly in reality, its amplitude will dominate in the two tide solution. The chosen range of NMT wave-numbers used is based on the theory that NMTs are generated by interaction between quasi-stationary planetary waves (QSPW), $S = 1$ or 2 (at Arctic latitudes), and the migrating tides (e.g. Forbes et al., 2003). Thus NMT wave-numbers are the MT wave number ± 1 or 2. The dominance of QSPW $S = 1$ and 2 in the Arctic was demonstrated in Paper 1, but also by recent assessment of Aura MLS temperatures; these latter results will be published elsewhere. Finally, the recent NMT results from Iimura et al. (2010), using the Thermosphere Ionosphere Mesosphere Energetics and Dynamics (TIMED) satellite with its Doppler Interferometer (TIDI), involved wave-numbers consistent with SPW $S = 1$ and 2.

We have used the MT/NMT amplitude ratios in these selected NMT wave-number ranges to determine the dominant tide: the MT is chosen if all ratios (from MT+NMT fits) are greater than 2 (black height-month squares in Fig. 3); or the wave-number "*s*" is chosen (for the squares in Fig. 3) for the NMT with the smallest MT/NMT ratio; except that an additional choice has been developed for the related figures in this paper (grey squares) for when the largest NMT tide is greater than 0.5 of the MT, but smaller than the MT. Such grey areas thus have the MT as the stronger wave, but a NMT is competitive.

Thus Fig. 3 shows diurnal tide MT and NMT choices from 12 monthly fits versus 6 heights (72 height-month locations) for each of years 2006/2007, 2007/2008 and 2008/2009. . . and for EW and NS tidal components. The sections of black/grey or named-NMT in Fig. 3, for 2006/2007, are identical to those in the figure of Paper 1, apart from the added useful indication of where the NMT is relatively close to the MT in amplitude; regularity or consistency in the data is confirmed by the strong tendency for the grey squares to be in clusters.

The immediately visible feature of inter-annual variability (IAV) in Fig. 3 is the dominance of the NMT $s = +2$ (effect

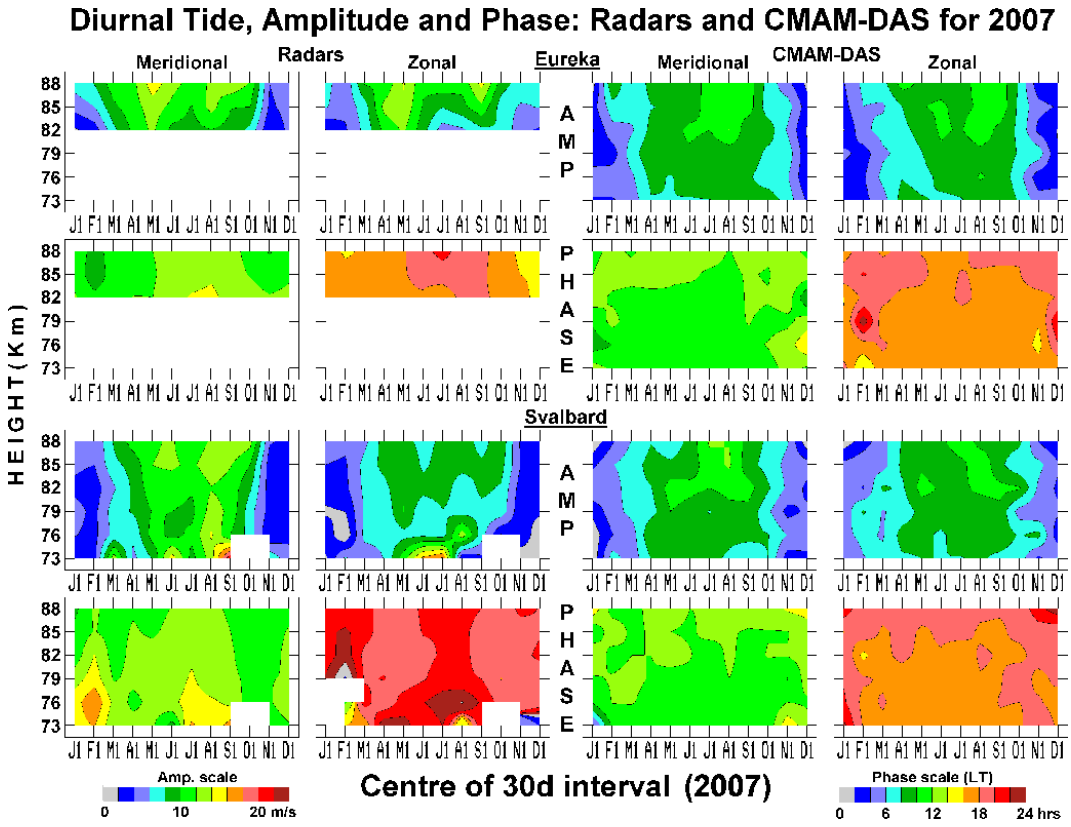

Fig. 4. Zonal (U, EW) and meridional (V, NS) winds for the diurnal (24-h) tides (DT) above Eureka and Svalbard for year 2007, from the two MWR and CMAM-DAS, and from the harmonic fits to the mean wind, 24- and 12-h tidal amplitudes and phases: the phases are the local solar times of maximum northward and eastward winds.

of QSPW $S = 1$) for NS and EW components in the spring of 2006. In contrast, the NS component of spring's 2007 and 2008 is dominated by the MT; while for the EW component the fall-early winter of 2006–2007 has the most dominant and coherent presence of the $s = 0$ NMT. The above is consistent with Fig. 2, where the Eureka DT-phases show very large spring 'variations' that are largely due to the spring of year 2006, with its unique dominance of NMT $s = 2$.

For the late autumn and winter months (November–February) of Fig. 3, and for the zonal component, NMT tides ($s = 0$) are significant or dominant for the three years. For the meridional component in these months, the $s = 2$ tide (also due to QSPW $S = 1$) is quite frequently seen in all three years, along with an NMT tide approaching the amplitude of the MT (grey boxes). The DT phase variations (Fig. 2) are relatively large in these months also.

It is interesting to know that the IAV of the DT amplitudes, over consecutive years, is very conspicuous and largest in the spring and winter. Also, the occurrence of NMTs is quite frequent, their seasonal variability has some regularity, and their variability often matches seasonal "variations" of the observed DT. As such, one has reason to be optimistic that a modern and physically complete GCM should reproduce some of these DT features: required middle atmosphere characteristics appear to be that the High Arctic tides are well forced and reproduced, and that the SPW are of significant strength and occurrence.

3.3 Comparisons of the 2007 arctic diurnal tides in CMAM-DAS with observed tides from MWR measurements

Height versus time contours of the modeled and observed diurnal tidal (DT) amplitudes and phases of a single year, 2007, are now assessed (Fig. 4): this year represents the frequent and special physical situation when the meridional winter-centred monthly mean winds at Svalbard are dominantly southward (Manson et al., 2011). In the plots we include radar-values up to 88 km, which is the highest height used from CMAM; on the other hand, and since the Svalbard-winds extend down to 73 km, CMAM values down to there are included for Svalbard-comparisons.

A quick comparison with the 3 year means of Fig. 1 is useful (the latter uses the same color code as Fig. 4): the observed Eureka and Svalbard DT amplitudes of 2007 are quite similar to the 3 year means; and the phases are generally similar in color, if not in all phase-transitions. Since

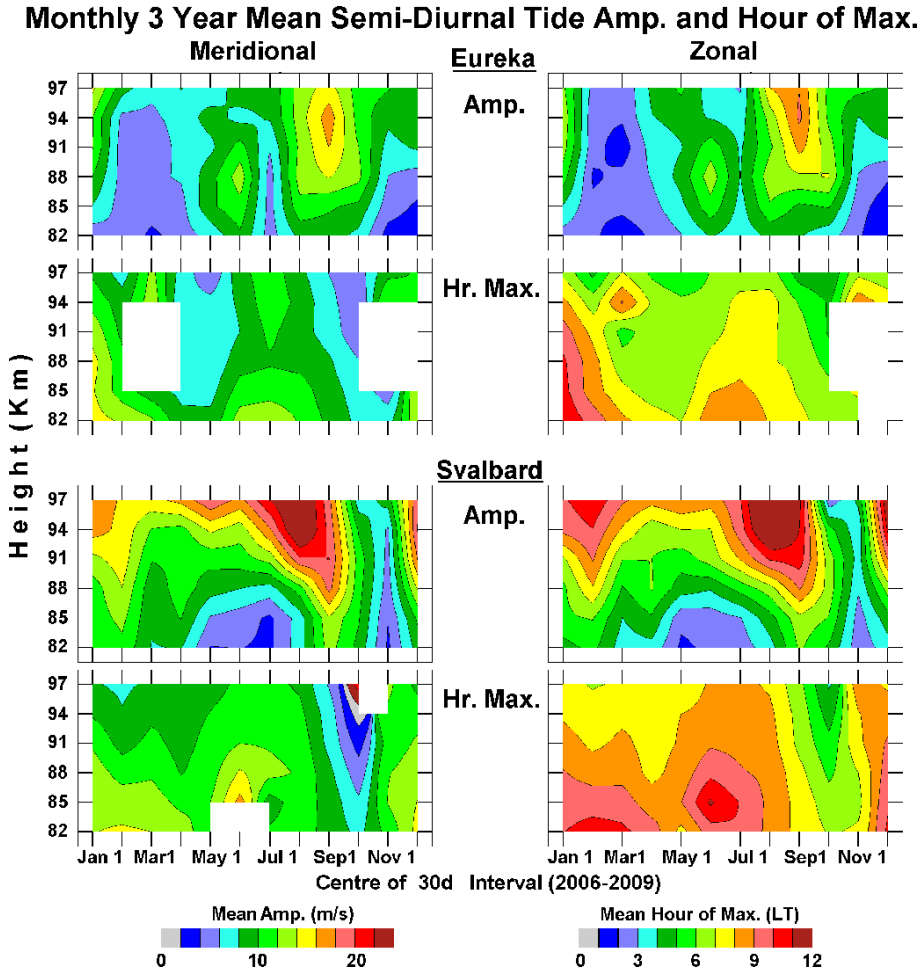

Fig. 5. Zonal (U, EW) and meridional (V, NS) winds for the semi-diurnal (12-h) tides (SDT) above Eureka and Svalbard for days February 2006–February 2009: the phases are the local solar times of maximum northward and eastward winds. Separate averaging for amplitudes and phases was done for the tides, and if the phase-spread between the values from three years exceeds 180° for an interval, a phase-gap is shown. 30-day fits are used, with the first day of the calendar month as the middle of the 30-day data sets.

these latter involve clear visual changes in color, we will use phrases such as "color transitions", as this is more informative of the basic mental experiences of the reader). Following careful scrutiny, observed Eureka-amplitudes have equinoctial maxima (May, September), while modeled amplitudes have a late summer-early autumn maximum in both components. Also, although observations and model at Eureka share similar colors for phases, the monthly sequencing of colors/phase is quite different. Components (NS, EW) as observed or modeled have similar amplitudes and phases-in-quadrature, appropriate for a circular tide, with clockwise rotation in time. Moving next to Svalbard, amplitudes of both components from radar and from model again show minima in winter-centered months; and there are no significant vertical gradients. Most seriously, and in non-winter months, while the observed NS amplitudes are circa twice the EW, the modeled components are close to being equal. Consistent with this, the radar provides elliptical (∼8 h differences rather than 6) or even linear oscillations (NS stronger), while model-components are, as at Eureka, in quadrature. Paper 1, using data from 2006, also showed that the tidal winds from Svalbard were elliptically polarized. Finally, although phases (for particular months and heights) from the radar and model are generally within one color difference (2 h) of each other, radar and model demonstrate (small) variations in time and height (model) that differ.

As was already noted in Sect. 3.2, the diurnal tides derived from the radars evidence significant NMT-effects i.e. location-dependant amplitudes and phases especially above 90 km (Fig. 1). The CMAM tides of Fig. 4 show much smaller locational differences, and hence fewer indications of NMT e.g. the NS-component amplitudes and phases at 86° W and 16° E are almost identical, as are the EW values.

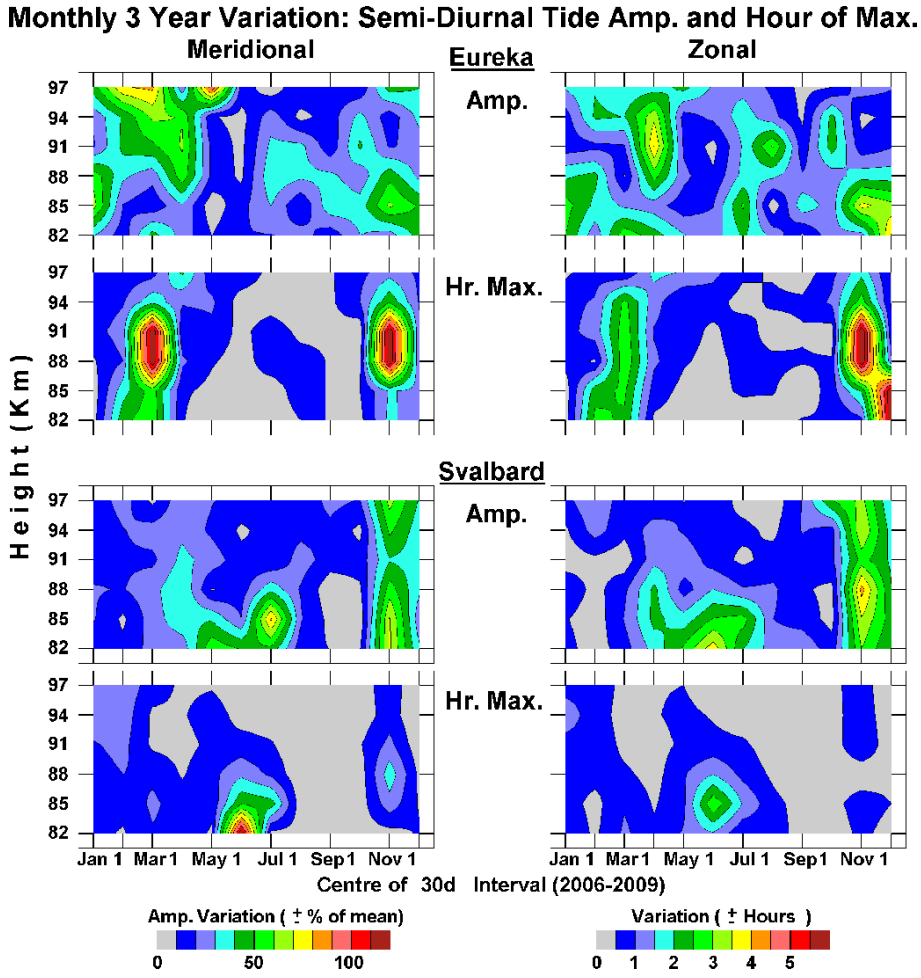

Fig. 6. The "variation" of 12-h tidal amplitudes and of phases (local times of maximum), over three years (February 2006 to February 2009), are provided. The "variation" of amplitude is [100(maximum − minimum)/(maximum + minimum)] %, and "variation" of phase is hours: [(maximum − minimum)/2]). Separate calculations for amplitudes and phases were done for the tides.

4 Semi-diurnal tides (2006–2009): migrating (MT) and non-migrating (NMT); comparisons with CMAM-DAS

4.1 Introduction

The "monthly 3 year mean" amplitudes and phases of the semi-diurnal (12-h) tides (SDT) for 2006–2009, at both locations, are provided in Fig. 5, with their "monthly 3 year variations" in Fig. 6. Otherwsie the methodologies used are as in Sect. 3.

4.2 Semidiurnal tides: means, variations and NMT features

At Eureka (Fig. 5) the minimum SDT amplitudes are in early and late winter months (November–December and February–March), with small maxima early in June and January and the broader major maximum centred early in September. Minima in "variation", the variable used for IAV here (Fig. 6), occur at the times of amplitude-maxima (June, September). The Eureka phases are consistently orthogonal (3 h differences). Vertical phase-gradients are largest in winter (equivalent to local vertical wavelengths λ of $\sim$30 km), modest in summer ($\lambda \sim 100$ km), and very long/evanescent in the equinoxes. "Variations" in Fig. 6 are very large at the winter-spring and autumn-winter transitions, consistent with indeterminate phases (Fig. 5) for the phase-contours; otherwise near the amplitude maxima (Fig. 5) the phase-variations are small ($\pm$1 h or less).

Turning to the Svalbard SDT (Fig. 5) the largest vertical extensions of the zonal and meridional maxima $\sim$85–97 km also occur in September, they are much larger ($\geq$22 m s^{-1} vs. 16–18 m s^{-1}) and peak earlier and higher (early August, 97 km) compared to Eureka. Due to this feature and also the larger winter maxima, the SDT at Svalbard is generally much larger than at Eureka. It is also the dominant

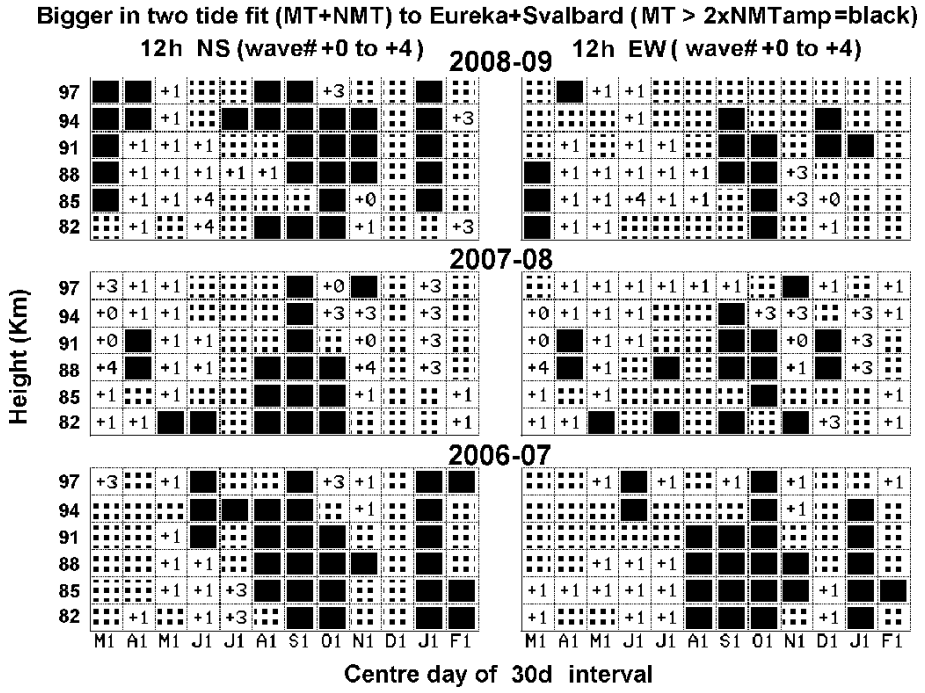

Fig. 7. Two-tide fits, using the wave number of the Semi-Diurnal MT ($s = 2$) plus one of a range of NMT, were used to find the relative sizes: a black square is chosen if MT is greater than twice any NMT value; a grey square is chosen when one or more NMT values are smaller then MT, but greater than 0.5 of MT; the wave-number "s" is chosen that has the largest NMT [relative to the corresponding MT amplitude] of all of the fits. Wave-numbers ($s = 0$ to $+4$) are appropriate to non-linear interaction with the SPW $S = 1$ or 2.

solar tide. Phases at Svalbard are orthogonal (a circularly rotating wind vector); and they have some temporal similarity of color/phase-patterns with Eureka. There are strong phase-changes at Svalbard (82–97 km) from August to November, with re-establishment of moderate vertical gradients (equivalent $\lambda \sim 70$ km) by early winter. Moreover, these phase-gradients of winter are maintained through the spring, whereas at Eureka the equivalent wavelengths are evanescent.

The SDT mean amplitudes and phases for 2006–2009, as shown in Fig. 5, indicate significant and probably very frequent presence of NMT. Amplitudes differ greatly between the radar-locations and phases agree only occasionally. Figure 7 is the counter-part of Fig. 3 for the SDT. The format and available information is the same, with height-month squares of the dominant NMT (with choice of values determined by SPW $S = 1, 2$), black for the dominance of MT, or grey when a NMT is greater than 0.5 of the MT. The addition of the "grey" condition is very valuable as it confirms the qualitative assessment of Fig. 5, since the MT (black boxes) is dominant almost exclusively during the September–October events of each of the three (3) years; and black/grey is relatively common in winter. The dominance of NMT $s = +1$ at the lower heights of the mesosphere, and for spring/early-summer, continues from 2006/2007 as the outstanding feature. The cause of this remains unknown and puzzling, as the SPW activity ($S = 1$) has by then become modest... there will be discussion of this in the final section of the paper.

Inter-annual variability (IAV) of the occurrence of MT and NMT is well demonstrated in Fig. 7. Some examples are these: the IAV is significant in winter months, with the 2006/2007-year having the clearest evidence for MT dominance; 2007/2008 showing more preference for NMT $s = 3$ (also associated with SPW $S = 1$) than other years; and 2008/2009 favoring frequent occurrences of large but not dominant MT (grey), especially in the EW component.

We appreciate that one of the referees informed us, during the late stages of the reviewing process, of the recent paper by Iimura et al. (2010), using data from TIMED-TIDI, which provided unique satellite Arctic NMT information for the SDT: mainly the westward propagating wave-numbers $s = +1, +3$, and standing wave number $s = 0$. The $s = +1$ was most prominent ($\sim 10\,\mathrm{m\,s^{-1}}$), 90 to ~ 105 km, for months mid-March to mid-May, and reaching the high Arctic (80–87° N). This agrees well with our Fig. 7, where $s = +1$ dominates in the spring. The NMT $s = 0$ from TIDI was much weaker at 80° N, consistent with Fig. 7 having few $s = 0$ values. The $s = +3$ of Fig. 7 occur mainly in months October–November and January–February, which is similar to the TIDI-NMT data. These TIDI tidal data are consistent with the dominance of SPW $S = 1$, as also indicated by the radar data of this paper. Overall the comparison is good; and

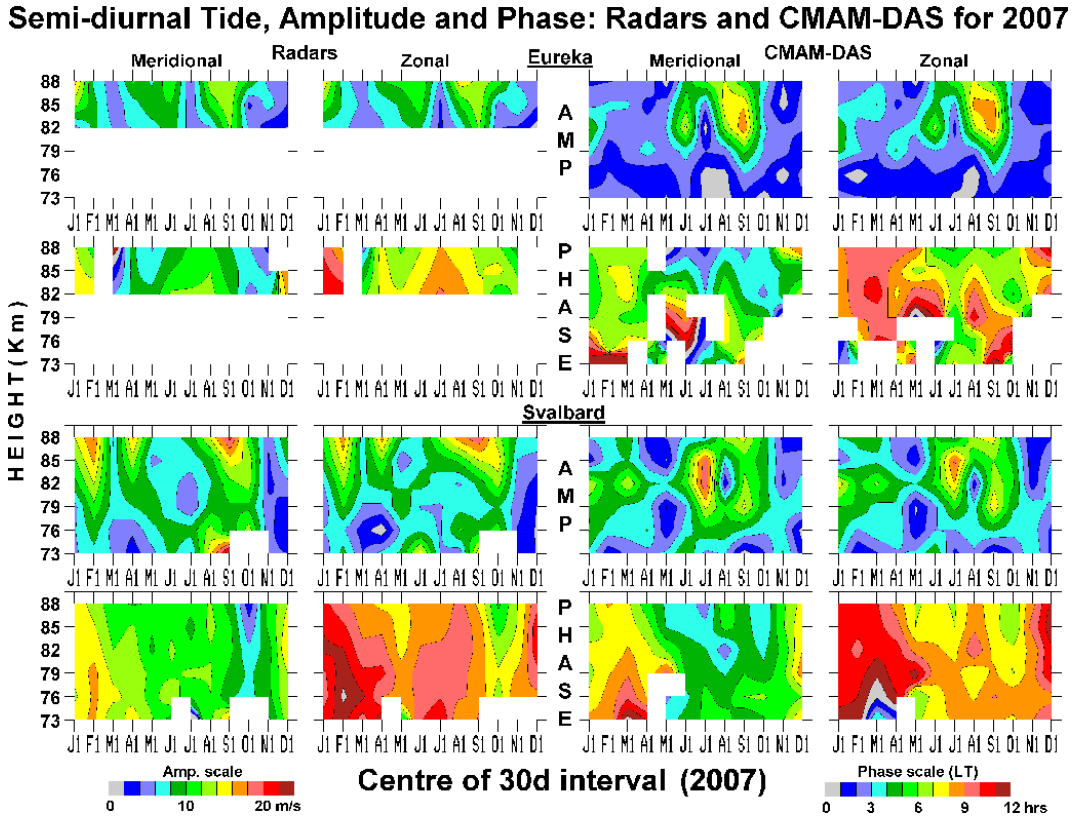

Fig. 8. Zonal (U, EW) and meridional (V, NS) winds for the semidiurnal (12-h) tides (SDT) above Eureka and Svalbard for year 2007 from the two MWR and CMAM-DAS, and from the harmonic fits to the mean wind, 24- and 12-h tidal amplitudes and phases: the phases are the local solar times of maximum northward and eastward winds.

this paper no longer provides almost solitary substantial information on the SDT NMT of the high Arctic!

Our studies of the stratospheric winter polar vortex illustrate the tendency for the SPW $S = 1$ to be dominant at these Arctic latitudes (e.g. Xu et al., 2009a, b), as was the case for 2006/2007 (Paper 1). This is consistent with the prevalence of anticyclones to form in the Pacific-Western Canada longitudinal sector, and the cyclone to be resident over Scandinavia (Manson et al., 2008, 2011; Xu et al., 2009b).

4.3 Comparisons of the Arctic semi-diurnal tides (2007) in CMAM-DAS with observed tides from meteor radars

The raison d'etre is the same as in Sect. 3.3: assessment of the middle and late months of winter 2006/2007, when the meridional winter-centred monthly mean winds over Svalbard were anomalous due to their dominantly southward flows (e.g. Paper 1). This, as the net northward meridional flows are responsible for downward polar mesospheric motions and adiabatic winter heating in the high Arctic.

Figure 8 for the 2007 SDT provides observed tides quite similar to the three year means (Fig. 5), but with both radars showing more variability and structure in the contoured amplitudes and phases (colors and their vertical gradients) in late winter-early spring (January–March) than the 3 year means. Comparing now the radar and CMAM panels of Fig. 8 for Eureka, amplitude-maxima above ∼80 km occur at the same times (June and September), although the observed maxima close or are still open at greater heights (88–97 km). The Eureka phases show considerable system-based differences, with the modeled values showing seasonal, monthly and altitudinal differences from those observed. Modeled values are also more variable in temporal and spatial scales.

For Svalbard, amplitudes of both components from radar and from model again show strong differences: observed maxima occur at upper heights (79–97 km; data for 91–97 km are outside the boundaries of Fig. 8) for late winter-spring and for the September-feature (Manson et al., 2010); while the equivalent modeled features are at lower heights (centered at 82 km) in summer and September. Phases, while internally consistent (EW and NS rotation sense; seasonal changes), differ quite strongly between observations and model.

From the above assessments and Fig. 8, there are generally significant differences between the observed SDT amplitudes and phases at Eureka and Svalbard. The CMAM tides show

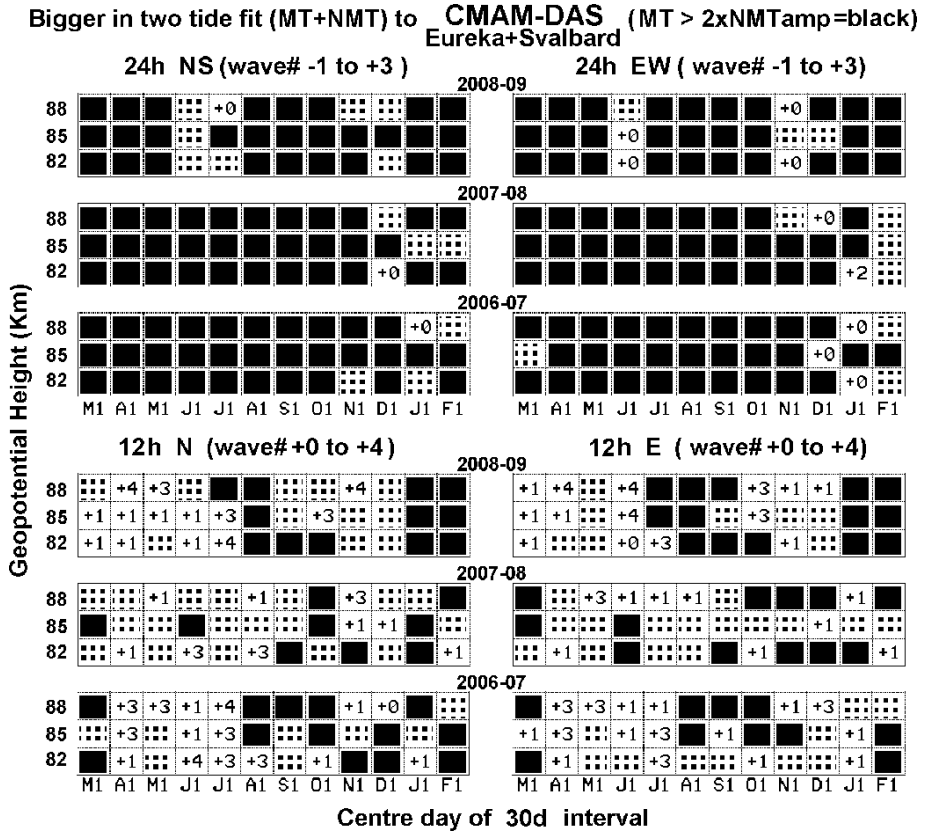

Fig. 9. Two-tide fits to the CMAM-DAS data for three separate years, using the wave number of the diurnal MT (DT, $s = 1$) plus one of a range of NMT (top set of plots), and semidiurnal MT (SDT, $s = 2$) plus one of a range of NMT (bottom set of plots), were used to find the relative sizes: a black square is chosen if MT is greater than twice any NMT value; a grey square is chosen when one or more NMT values are smaller then MT, but greater than 0.5 of MT; the wave-number "s" is chosen that has the largest NMT [relative to the corresponding MT amplitude] of all of the fits. Wave-numbers ($s = -1$ to $+3$) for the DT and ($s = 0$ to $+4$) for the SDT are appropriate to non-linear interaction with the SPW $S = 1$ or 2.

even more frequent site/locational differences. However the September feature does share similar amplitudes and appropriate phases at each site, and for each component. Thus the MT is expected to dominate there, with significant NMT presence in other months.

5 Plots of monthly mesospheric MT and NMT preferences (2006–2009) for DT and SDT from CMAM-DAS

Observed site-differences for DT and SDT were discussed in Sects. 3 and 4, leading to "box-plots" of MT/NMT amplitude ratios (height versus month) for both diurnal and semidiurnal tides (Figs. 3 and 7) and for each month of 2006–2007, 2007–2008 and 2008/2009. Dominant NMT values were provided; there were also black boxes when the MT dominated and gray-boxes when the NMT was smaller than, but comparable to, the MT (actually NMT > 0.5 MT).

In Fig. 9 we repeat this exercise for the DT and SDT of CMAM. As expected from Sect. 3, where very modest modeled site-differences were noted (Fig. 4) for the diurnal tide of 2007, the height-month MT/NMT boxes are generally dominated by the MT-black in Fig. 9. We have used the same 30-day sequences (March 2006 to February 2007) as in the MT/NMT box-plots for the observed tide (Fig. 3), for ease of comparison by the reader. The CMAM-DAS model does have a somewhat weaker preference (gray, black) for MT in the winter months (December–February) of 2006/2007 and 2007/2008, and $s = 0$ is preferred when a NMT wave-number dominates. Meanwhile, the observed winter-atmosphere had much greater NMT presence (Fig. 3), with wavenumber $s = 0$ strongly favoured for the EW component and $s = 2$ to a lesser extent for the NS component. Combined with the larger occurrence of NMT in non-winter months (gray height-month boxes), the observed atmosphere is generally richer in diurnal NMT (and therefore the associated QSPW) than the CMAM atmosphere, for years 2006–2009.

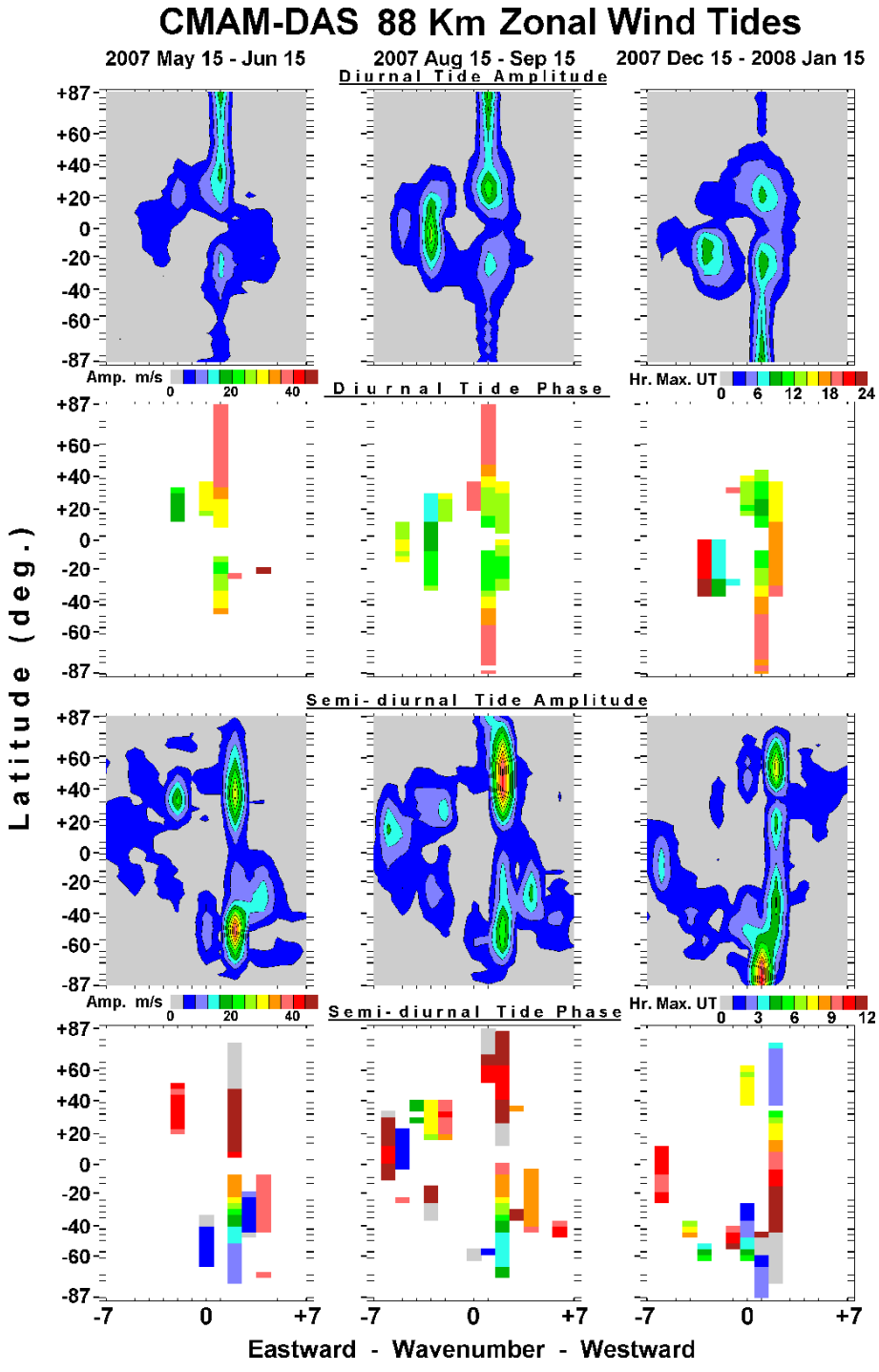

Fig. 10. Contour-plots of amplitudes and phases of the zonal wind diurnal and semidiurnal tides as functions of wave-number (positive for westward propagation) and latitude (positive for Northern Hemisphere): data for near the summer and winter solstices along with the boreal autumn for the model CMAM-DAS have been used, and the results for 88 km are shown. Phase is the hour of maximum (UT) at the Greenwich Meridian. For clarity, a phase value is just shown when its corresponding amplitude is above an arbitrary threshold.

As expected from Sect. 4.2 where quite frequent modeled site-differences were noted (Fig. 8) for the semi-diurnal tide of 2007, the height-month MT/NMT boxes of Fig. 9 are dominated by grey or a named-NMT wavenumber (22 of 36 choices per year), with relatively fewer indications of MT dominance. There is also a weaker tendency for MT to

preferentially appear during the occurrence of the modeled September-feature (Fig. 9) than in the corresponding figure for observations (cf. Fig. 7). In conclusion, consistent with the appearance of the SDT in Fig. 8, the plots for the 3-years of modeled MN/NMT ratios (Fig. 9) are generally noisier, or more random, than in the figure using the radar-observations (cf. Fig. 7).

6 High-Arctic latitude wave-number spectra for MT and NMT

In previous sections some comparisons between tides produced from radar observations and from CMAM-DAS model have been provided. Here we show another analysis that allows further assessments of MT and NMT features.

Figure 10 provides CMAM-derived wave-number spectra for 30 days centered on seasonally representative days: 1 June and 1 September 2007, as well as on 1 January 2008. The zonal/EW component of the diurnal (top) and semidiurnal (bottom) tides at 88 km are provided. Central dates ∼20 days before the summer-solstice and equinox are shown: 1 June and 1 September are also appropriate due to SDT amplitude maxima (Figs. 5 and 8) both observed and modeled; and the DT (Figs. 1 and 4) has indications of equinoctial maxima, from the radars and CMAM. Otherwise monthly amplitudes and phases in wavelets (not shown) change little from June/December to July/January.

For the diurnal tide, the MT $s=+1$ of the two summer solstices (16–20 m s^{-1}) dominate those of the two winter solstices (4–8 m s^{-1}), as expected, at Polar Arctic and Antarctic latitudes from ∼65–87° N/S. NMT play a minor role (<4 m s^{-1}) in all three months of CMAM, with no other resolved features at these high latitudes of either hemisphere. We restrict ourselves now to features relevant to the Polar latitudes and those that are not classical in nature. Phases are very similar in Northern and Southern Hemispheres (NH and SH) for the equinoxes (symmetric Hough-modes probably dominate). For no 30 d interval are the NH and SH amplitudes equal for the Boreal (September–October) autumn, likely due to hemispheric asymmetries in land/ocean areas and related atmospheres. Diurnal NMT are significant only at equatorial and sub-tropical latitudes (Manson et al., 2004a; Forbes et al., 2003). The above highlights are reasonably consistent with the MWR and CMAM-DAS diurnal tide comparisons in Fig. 4, and also the NMT and MT height-time occurrences discussed using Fig. 9. That is: the NMT are much less evident in the model than from observations. For the latter $s=0$, as forced by a QSPW $S=1$, significant prominence for the NMT exists (Fig. 3).

The semidiurnal tide (SDT) spectra of Fig. 10 illustrate the expected solstitial asymmetries for MT $s=2$ in Boreal-summer and Austral-winter, and vice versa. Also the SDT is less affected by hemispheric differences in solstitial solar radiation than the DT, with summer amplitudes not dominating those of winter. Such is also the case (albeit in more complex fashion) at the two radar locations (Fig. 9) and has been long recognized at middle latitudes (Manson et al., 2006). For the solstices in Fig. 10, the NMT $s=-2$ is outstanding only at middle latitudes in the Boreal summer. For the August/September months at mid-latitudes the $s=-2$ and $s=+4$ (related to SPW $S=4$ and 2) are shown for NH and SH respectively (see also Manson et al., 2004a, b; 2010).

For southern and northern polar regions there are striking SDT spectral features from CMAM data (Fig. 10), in particular the NMT $s=+1$ (related to SPW $S=1$) in the southern summer. This feature has also been observed, as noted in the Introduction (Paper 1; Hibbins et al., 2010; Xu et al., 2009a, c; Murphy et al., 2009; Baumgaertner et al., 2005, 2006). These 3 groups of authors also demonstrate that there are significant correlations and probable causal linkages between the SPW $S=1$ of the NH-winter and both the directly observed winter-SDT and the related NMT $s=+1$ of the SH-summer. For the winter of the SH, the spectra of Fig. 10 show no indication of NMT $s=+1$ in the NH. This negative indication has been variously reported in the above papers; and the most recent paper by Hibbins et al. (2010) sheds fresh insights on the seasonal and longitudinal variations of this NMT of the SH. In the NH, the spectral presence of NMT $s=+1$, from CMAM global data (Fig. 10), is only evident in the autumn. However, when data are sampled only at the Eureka and Svalbard locations, the indications of NMT $s=+1$ are weak in Fig. 9 (from CMAM data) and very weak from the independent radar data (Fig. 7).

7 Summary and discussion

The discussions throughout this paper have been quite detailed, so we will not extend them unduly here. A few observations in summary/discussion are expected however. Generally the items below follow the sections of the paper and their findings; and these main emphases ("goals") have been provided in the last paragraph of the Introduction: assessments of the interannual variations (IAV) in the character of the tides, migrating and (uniquely) non-migrating; and the first substantial comparisons between the High Arctic observations from the Meteor Winds Radars (MWR) and the model CMAM-DAS.

1. The first 36 months of wind-data (82–97 km) from the Meteor (Winds) Radar (MWR) at Eureka, Ellesmere Island (80° N, 86° W), within the PEARL-CANDAC laboratory, have been here combined with contemporaneous winds from the Meteor Radar at Adventdalen, Svalbard (78° N, 16° E). The combined data archive is from mid-February 2006 to February 2009. This has been used to provide the first significant characterization of the IAV of longitudinally spaced observations of tides at such "High Arctic" latitudes. This unique Arctic

archive involves the diurnal and semidiurnal migrating (MT) and non-migrating tides (NMT).

2. The observed monthly means for both diurnal (D) and semi-diurnal (SD) tidal winds of the upper middle atmosphere demonstrate significantly different magnitudes and phases at Eureka and Svalbard. This confirms the longitudinal differences first seen with the 2006 data (Paper 1). Typically the summer-maximizing DT winds are larger at Eureka ($24\,m\,s^{-1}$ at 97 km versus $5–24\,m\,s^{-1}$), while the Svalbard tides are almost linearly polarized (north-south) rather than circular. Phase time-sequences are consistent with large or evanescent vertical wavelengths. Inter-annual variations (IAV) are largest in the winter and spring months. The Arctic SDT winds have maxima centred on August/September, followed in size by the winter features, and are much larger and temporally extended at Svalbard than at Eureka ($24\,m\,s^{-1}$ at 97 km, versus $14–18\,m\,s^{-1}$). Main features for the IAV, which have temporal and altitudinal characteristics, are in spring and winter at Eureka, and early summer and late autumn at Svalbard.

   Given the evidence (Manson et al., 2011) for systematic (2006–2009) polar vortex-distortions representing longitudinal wind-asymmetries in the winter-months of the NH, quasi-stationary planetary waves (QSPW or SPW) are necessarily relatively large i.e. compared to Antarctica. The SPW lead to longitudinal tidal structures of amplitude and phase, which have the scales of the dominant SPW ($S = 1$ and 2) (Manson et al., 2004a and b; Forbes et al., 2003; Cierpik et al., 2003). It is therefore possible for radars to have been located, by the chances provided for available land, so that positive, negative or minimal correlations (in time) are found between observed tides and the SPW (Baumgaertner et al., 2006; Xu et al., 2009a, c; Hibbins et al., 2010).

3. Fitting of wave numbers for the migrating and non-migrating tides (MT, NMT), assuming the dominance of QSPW ($S = 1$ and 2), has been used to determine the dominant tides for each month and height, now over three years. Inter-annual variations for the tides have emerged from this analysis. For the diurnal oscillations, NMT $s = 0$ for the east-west (EW) wind component dominate in size (largest tide) and occurrence in each of the late autumn and winter months (November–February). Wave-number $s = +2$ was seen in the NS component for the same months of 2006/2007. These NMT are consistent with interactions with stationary planetary wave (SPW) $S = 1$, which generally dominate the SPW spectrum at these latitudes (Manson et al., 2009). It is interesting that the distance between Svalbard and Eureka is ∼2400 km, relatively close to 90° (2100 km) for the $S = 1$ SPW. Thus Eureka, with the larger observed tide, appears to be closer to the maximum of the spatially modulated observed tide (item 2 above), while Svalbard is closer to the location where minimal effect of the NMT upon the observed tide amplitude occurs.

   For the semi-diurnal oscillation, NMT $s = +1$ dominated (size and occurrence) both EW and NS components of the wind from March to June/July of the three years. There were also autumn months (August–October), for each year (2006–2009), when the MT was generally dominant. This latter is associated with the "September" feature (30°–70°), which is dominated by the MT (Manson et al., 2010). Generally, over the three years, the NMT was either dominant, or comparable to the MT, 77 % of the available month-height possibilities. Late in the reviewing process a referee provided us with the Iimura et al. (2010) reference; their paper, using TIMED-TIDI data, provided SDT NMT values for the high Arctic (circa 80° N). The resulting dominance of $s = +1$ in the spring, and the weaker $s = +3$ in fall and winter are in good agreement with the NMT results reported here, originating from the two MWR radars.

4. Comparison of observed DT and SDT at 78–80° N, with those within CMAM-DAS, is a major feature of this paper. Given the significant inter-annual variability, the year 2007 was chosen, to best represent features that we recognize as typical of the dynamics at these two locations.

   The diurnal tides for the two locations have significant similarities as observed and modeled, with seasonal maxima in the mesosphere from April to October, and similar phases with inferred long/evanescent wavelengths. Differences between MWR and CMAM DT are also very significant: observed amplitudes are generally larger than modeled, especially at Eureka; modeled phases (NS, EW) are classically similar at Eureka and Svalbard, with circular/orthogonal wind components, while the observed tide is approximately circular at Eureka, but close to linear (∼NS direction) at Svalbard. Given the lack of significant modeled locational (86° W and 16° E) tidal differences, it is not surprising that the occurrence of NMT in the model is much weaker than observed. The reasons for modeled tide discrepancies are likely to be numerous and would require considerable diagnosis/experiments with CMAM-DAS global atmospheres. Factors, many of which are known to differ from planet Earth, would involve tidal sources (heights and latitudes), background winds and meridional temperature gradients, as well as wave-drag (PW in the lower, GW in the upper altitudes) and turbulence.

   For the semi-diurnal tide, the modeled/observed pairs of amplitude and phase contour-plots (height versus month for a year) are generally dissimilar at the two

locations; as are modeled and observed plots at each of the two sites separately. The hemispheric "September" feature is the only frequent exception in such comparisons. Modeled time-variability of amplitude and phase on these plots is typically of higher frequency than that observed i.e. some observed structures, in particular the "September feature", have time-scales of more than two months. Further, the comparative noisiness of the modeled SDT data leads to less clustering of NMT or MT into common values than observed. Explanations for such differences between model and observation are not going to be easy to find, a better word is daunting, but comparisons of heating due to ozone and water vapor would be a useful place to start. Also desirable would be the same factors that affect the DT, but including the "September "feature peculiar to the SDT.

There are other interesting features of the tides observed by the radars at Svalbard and Eureka. Some of these were already apparent as we began this paper e.g. frequent amplitude-modulation of the tides for brief intervals (a few days), and the apparent disappearance of tidal oscillations for a few days. Others have appeared during this study. They will require considerable attention and time to fully explore, and will be considered elsewhere.

Acknowledgements. We are grateful to these: the University of Toronto, for access to the IPY archive and Michael Neish, for CMAM-DAS data with 1-h spacing. The Canadian Network for the Detection of Atmospheric Change (CANDAC), along with its Principal Investigator Professor James Drummond, is thanked profoundly for the provision of salary support (CEM, XX) and for the operation and maintenance of the radar at Eureka (Polar Environment Atmospheric Research Laboratory, PEARL). The Canadian authors acknowledge research support through grants from the Natural Sciences and Engineering Council (NSERC), research funding from the Canadian Foundation for Climate and Atmospheric Science (CFCAS), and support from their individual Universities, Departments and Institutes: in particular the Institute of Space and Atmospheric Studies (ISAS), University of Saskatchewan.

Topical Editor C. Jacobi thanks Q. Wu and another anonymous referee for their help in evaluating this paper.

References

Baumgaertner, A. J. G., McDonald, A. J., Fraser, G. J., and Plank, G. E.: Long-term observations of mean winds and tides in the upper mesosphere and lower thermosphere above Scott Base, Antarctica, J. Atmos. Solar-Terr. Phys. 67, 1480–1496, 2005.

Baumgaertner, A. J. G., Jarvis, M. J., McDonald, A. J., and Fraser, G. J.: Observations of the wave number 1 and 2 components of the semi-diurnal tide over Antarctica, J. Atmos. Solar-Terr. Phys., 68, 1195–1214, 2006.

Cierpik, K. M., Forbes, J. M., Miyahara, S., Miyoshi, Y., Fahrutdinova, A., Jacobi, C., Manson, A. H., Meek, C., Mitchell, N. J., and Portnyagin, Y.: Longitude variability of the solar semidiurnal tide in the lower thermosphere through assimilation of ground-and space-based wind measurements, J. Geophys. Res., 108, 1202, doi:10.1029/2002JA009349, 2003.

Forbes, J. M. and Wu, D.: Solar tides as revealed by measurements of mesosphere temperature by the MLS experiment on UARS, J. Atmos. Sci., 63, 1776–1797, 2006.

Forbes, J. M., Makarov, N. A., and Portnyagin, Y.: First Results from the Meteor Radar at South-pole – A large 12-hour Oscillation with Zonal wave-number one, Geophys. Res. Lett., 22, 3247–3250, 1995.

Forbes, J. M., Zhang, X. L., Talaat, E. R., and Ward, W.: Nonmigrating diurnal tides in the thermosphere, J. Geophys. Res.-Space Physics, 108, 1033, doi:10.1029/2002JA009262, 2003.

Hagan, M. E. and Forbes, J. M.: Migrating and nonmigrating semidiurnal tides in the upper atmosphere excited by tropospheric latent heat release, J. Geophys. Res.-Space Physics, 108, 1062, doi:10.1029/2001JD001236, 2003.

Hall, C. M., Aso, T., Manson, A. H., Meek, C. E., Nozawa, S., and Tsutsumi, M.: High-latitude mesospheric mean winds: A comparison between Tromso (69° N) and Svalbard (78° N), J. Geophys. Res.-Atmos., 108, 4598, doi:10.1029/2003JD003509, 2003.

Hernandez, G., Fraser, G. J., and Smith, R. W.: Mesospheric 12-hour Oscillation near South-pole, Antarctica, Geophys. Res. Lett., 20, 1787–1790, 1993.

Hibbins, R. E., Marsh, O. J., McDonald, A. J., Fraser, G. J., and Plank, G. E.: A new perspective on the longitudinal variability of the semidiurnal tide, Geophys. Res. Lett., 37, L14804, doi:10.1029/2010GL044015, 2010.

Hocking, W. K. and Hocking, A.: Temperature tides determined with meteor radar, Ann. Geophys., 20, 1447–1467, doi:10.5194/angeo-20-1447-2002, 2002.

Iimura, H., Fritts, D. C., Wu, Q., Skinner, W. R., and Palo, S. E.: Nonmigrating semidiurnal tide over the Arctic determined from TIMED Doppler Interferometer wind observations, J. Geophys. Res.-Atmos., 115, D06109, doi:1029/2009JD012733, 2010.

Manson, A. H., Meek, C. E., Chshyolkova, T., Avery, S. K., Thorsen, D., MacDougall, J. W., Hocking, W., Murayama, Y., Igarashi, K., Namboothiri, S. P., and Kishore, P.: Longitudinal and latitudinal variations in dynamic characteristics of the MLT (70–95 km): a study involving the CUJO network, Ann. Geophys., 22, 347–365, doi:10.5194/angeo-22-347-2004, 2004a.

Manson, A. H., Meek, C., Hagan, M., Zhang, X., and Luo, Y.: Global distributions of diurnal and semidiurnal tides: observations from HRDI-UARS of the MLT region and comparisons with GSWM-02 (migrating, nonmigrating components), Ann. Geophys., 22, 1529–1548, doi:10.5194/angeo-22-1529-2004, 2004b.

Manson, A. H., Meek, C. E., Hall, C. M., Nozawa, S., Mitchell, N. J., Pancheva, D., Singer, W., and Hoffmann, P.: Mesopause dynamics from the scandinavian triangle of radars within the PSMOS-DATAR Project, Ann. Geophys., 22, 367–386, doi:10.5194/angeo-22-367-2004, 2004c.

Manson, A. H., Meek, C., Chshyolkova, T., McLandress, C., Avery, S. K., Fritts, D. C., Hall, C. M., Hocking, W. K., Igarashi, K., MacDougall, J. W., Murayama, Y., Riggin, C., Thorsen, D., and Vincent, R. A.: Winter warmings, tides and planetary waves: comparisions between CMAM (with interactive chemistry) and MFR-MetO observations and data, Ann. Geophys., 24, 2493–2518, doi:10.5194/angeo-24-2493-2006, 2006.

Manson, A. H., Meek, C. E., and Chshyolkova, T.: Regional stratospheric warmings in the Pacific-Western Canada (PWC) sector during winter 2004/2005: implications for temperatures, winds, chemical constituents and the characterization of the Polar vortex, Ann. Geophys., 26, 3597–3622, doi:10.5194/angeo-26-3597-2008, 2008.

Manson, A. H., Meek, C. E., Chshyolkova, T., Xu, X., Aso, T., Drummond, J. R., Hall, C. M., Hocking, W. K., Jacobi, Ch., Tsutsumi, M., and Ward, W. E.: Arctic tidal characteristics at Eureka (80° N, 86° W) and Svalbard (78° N, 16° E) for 2006/07: seasonal and longitudinal variations, migrating and non-migrating tides, Ann. Geophys., 27, 1153–1173, doi:10.5194/angeo-27-1153-2009, 2009.

Manson, A., Meek, C., and Xu, X.: Comment on "Global structure, seasonal and interannual variability of the migrating semidiurnal tide seen in the SABER/TIMED temperatures (2002–2007)" by Pancheva et al. (2009), Ann. Geophys., 28, 665–676, doi:10.5194/angeo-28-665-2010, 2010.

Manson, A. H., Meek, C. E., Xu, X., Aso, T., Drummond, J. R., Hall, C. M., Hocking, W. K., Tsutsumi, M., and Ward, W. E.: Characteristics of Arctic winds at CANDAC-PEARL (80° N, 86° W) and Svalbard (78° N, 16° E) for 2006–2009: radar observations and comparisons with the model CMAM-DAS, Ann. Geophys., 29, 1927–1938, doi:10.5194/angeo-29-1927-2011, 2011.

Murphy, D. J., Forbes, J. M., Walterscheid, R. L., Hagan, M. E., Avery, S. K., Aso, T., Fraser, G. J., Fritts, D. C., Jarvis, M. J., McDonald, A. J., Riggin, D. M., Tsutsumi, M., and Vincent, R. A.: A climatology of tides in the Antarctic mesosphere and lower thermosphere, J. Geophys. Res.-Atmos., 111, D23104, doi:10.1029/2005JD006803, 2006.

Murphy, D. J., Aso, T., Fritts, D. C., Hibbins, R. E., McDonald, A. J., Riggin, D. M., Tsutsumi, M., and Vincent, R. A.: Source regions for Antarctic MLT non-migrating semidiurnal tides, Geophys. Res. Lett., 36, L09805, doi:10.1029/2008GL037064, 2009.

Portnyagin, Y. I., Forbes, J. M., Makarov, N. A., Merzlyakov, E. G., and Palo, S.: The summertime 12-h wind oscillation with zonal wavenumber $s = 1$ in the lower thermosphere over the South Pole, Ann. Geophys., 16, 828–837, doi:10.1007/s00585-998-0828-9, 1998.

Portnyagin, Y. I., Solovjova, T. V., Makarov, N. A., Merzlyakov, E. G., Manson, A. H., Meek, C. E., Hocking, W., Mitchell, N., Pancheva, D., Hoffmann, P., Singer, W., Murayama, Y., Igarashi, K., Forbes, J. M., Palo, S., Hall, C., and Nozawa, S.: Monthly mean climatology of the prevailing winds and tides in the Arctic mesosphere/lower thermosphere, Ann. Geophys., 22, 3395–3410, doi:10.5194/angeo-22-3395-2004, 2004.

Ren, S., Polavarapu, S. M., and Shepherd, T. G.: Vertical propagation of information in a middle atmosphere data assimilation system by gravity-wave drag feedbacks, Geophys. Res. Lett., 35, L06804, doi:10.1029/2007GL032699, 2008.

Wu, Q., Killeen, T. L., Nozawa, S., McEwen, D., Guo, W., and Solomon, S. C.: Observations of mesospheric neutral wind 12-hour wave in the Northern Polar Cap, J. Atmos. Solar-Terr. Phys., 65, 971–978, 2003.

Wu, Q., Ortland, D. A., Killeen, T. L., Roble, R. G., Hagan, M. E., Liu, H. L., Solomon, S. C., Xu, J. Y., Skinner, W. R., and Niciejewski, R. J.: Global distribution and interannual variations of mesospheric and lower thermospheric neutral wind diurnal tide: 2. Nonmigrating tide, J. Geophys. Res.-Space Physics, 113, A05309, doi:10.1029/2007JA012543, 2008.

Xu, X., Manson, A. H., Meek, C. E., Chshyolkova, T., Drummond, J. R., Hall, C. M., Jacobi, Ch., Riggin, D., Hibbins, R. E., Tsutsumi, M., Hocking, W. K., and Ward, W. E.: Relationship between variability of the semidiurnal tide in the Northern Hemisphere mesosphere and quasi-stationary planetary waves throughout the global middle atmosphere, Ann. Geophys., 27, 4239–4256, doi:10.5194/angeo-27-4239-2009, 2009a.

Xu, X., Manson, A. H., Meek, C. E., Chshyolkova, T., Drummond, J. R., Hall, C. M., Riggin, D. M., and Hibbins, R. E.: Vertical and interhemispheric links in the stratosphere-mesosphere as revealed by the day-to-day variability of Aura-MLS temperature data, Ann. Geophys., 27, 3387–3409, doi:10.5194/angeo-27-3387-2009, 2009b.

Xu, X., Manson, A. H., Meek, C. E., Chshyolkova, T., Drummond, J. R., Riggin, D. M., Hall, C. M., Hibbins, R. E., and Tsutsumi, M.: Asymmetry in the inter-hemispheric planetary wave-tide link between the two hemispheres, J. Atmos. Solar-Terr. Phys., 71, 1899–1903, doi:10.1016/j.jastp.2009.07.011, 2009c.

Xu, X., Manson, A. H., Meek, C. E., Jacobi, Ch., Hall, C. M., and Drummond, J. R.: Mesospheric wind semidiurnal tides within the Canadian Middle Atmosphere Model Data Assimilation System, J. Geophys. Res., 116, D17102, doi:10.1029/2011JD015966, 2011a.

Xu, X., Manson, A. H., Meek, C. E., Riggin, D. M., Jacobi, Ch., and Drummond, J. R.,: Mesospheric wind diurnal tides within the Canadian Middle Atmosphere Model Data Assimilation System, J. Atmos. Solar-Terr. Phys., accepted, 2011b.